Available online at www.sciencedirect.com

ScienceDirect

Advances in Space Research 62 (2018) 317–325

ADVANCES IN SPACE RESEARCH (a COSPAR publication)

www.elsevier.com/locate/asr

Calibration of Swarm accelerometer data by GPS positioning and linear temperature correction

Aleš Bezděk [a,*], Josef Sebera [b], Jaroslav Klokočník [a]

[a] Astronomical Institute, Czech Academy of Sciences, Fričova 298, 251 65 Ondřejov, Czech Republic
[b] ESA/ESRIN, Via Galileo Galilei, 00044 Frascati, Italy

Received 8 December 2017; received in revised form 23 April 2018; accepted 24 April 2018
Available online 3 May 2018

Abstract

Swarm, a mission of the European Space Agency, consists of three satellites orbiting the Earth since November 2013. In addition to the instrumentation aimed at fulfilling the mission's main goal, which is the observation of Earth's magnetic field, each satellite carries a geodetic quality GPS receiver and an accelerometer. Initially put in a 500-km altitude, all Swarm spacecraft slowly decay due to the action of atmospheric drag. Atmospheric particles and radiation forces impinge on the satellite's surface and thus create the main part of the nongravitational force, which together with satellite-induced thrusts can be measured by space accelerometers. Unfortunately, the Swarm accelerometer data are heavily disturbed by the varying onboard temperature. We calibrate the accelerometer data against a calibration standard derived from observed GPS positions, while making use of the models to represent the forces of gravity origin. We show that this procedure can be extended to incorporate the temperature signal. The obtained calibrated accelerations are validated in several different ways; namely by (i) physically modelled nongravitational forces, by (ii) intercomparison of calibrated accelerometer data from two Swarm satellites flying side-by-side, and by (iii) good agreement of our calibrated signals with those released by ESA, obtained via a different approach for reducing temperature effects. Finally, the presented method is applied to the Swarm C accelerometer data set covering almost two years (July 2014–April 2016), which ESA recently released to scientific users.

Keywords: Space accelerometers; Nongravitational accelerations; Swarm mission

1. Introduction

The European Space Agency (ESA) launched the three Swarm satellites on 22 November 2013, the main goal of the mission is a thorough study of the Earth's magnetic field (Friis-Christensen et al., 2008). Since then, the Swarm three-satellite constellation has provided a wealth of data, the scientific results from the first two years of the missions across the disciplines are summarized in a special journal issue (Olsen et al., 2016). Newest results based on Swarm observations were presented at the Swarm science meeting in Banff, Canada, in March 2017 (presentations available at http://www.swarm2017.org). The nominal duration of the Swarm mission was planned to be 4 years. The mission's successful global Earth mapping has recently been recognized by ESA member states; following an independent expert review, the Earth Observation Programme Board decided about the extension of Swarm until the end of 2021 (for more information and mission updates, see http://earth.esa.int/swarm/).

Besides the magnetic and electric field instruments, each Swarm satellite carries a GPS receiver and an accelerometer. The onboard geodetic quality *GPS receivers* have proved to be useful not only for a necessary positioning

* Corresponding author.
E-mail addresses: bezdek@asu.cas.cz (A. Bezděk), josef.sebera@esa.int (J. Sebera), jklokocn@asu.cas.cz (J. Klokočník).

https://doi.org/10.1016/j.asr.2018.04.041
0273-1177/

of Swarm satellites, but they also provided interesting material for dedicated studies on ionospheric disruptions in the GPS signals (Xiong et al., 2016) or they have been used to compute the temporal variations of the Earth gravity field (e.g. Bezděk et al., 2016; Encarnação et al., 2016; Dahle et al., 2017). Space *accelerometers* are designed to measure the nongravitational forces, whose action is localized on the satellite surface. For satellites in low Earth orbits (altitudes of 200–2000 km), the external physical nongravitational forces are dominated by atmospheric drag and solar radiation pressure. The solar radiation is coming directly from the Sun, but it has also components reflected from the Earth (albedo effect and thermal radiation). Additionally, accelerometers are also sensitive to the accelerations caused by onboard thrusters, which are activated occasionally (typically, a few times per day), when the control torque of the magnetic torquers is not sufficient to maintain the nominal attitude. For more information about the character of Swarm accelerometer data, we refer the reader to Bezděk et al. (2017, sect. 1.1). From the measured drag one can obtain the density of the neutral atmosphere, a quantity currently studied extensively in order to improve its models both for better knowledge of the near-Earth physics and for improved predictions of satellite orbits (e.g. Bruinsma et al., 2014; Visser et al., 2013).

The problem of the accelerometer data from the three Swarm satellites is an unusually high number of hardware-related anomalies (jumps, steps, etc.) and a large temperature dependence (Siemes et al., 2016; Bezděk et al., 2017). From the Swarm accelerometers, the least disrupted accelerometer data is collected by Swarm C, followed by Swarm A; their measured accelerometer signal can be decomposed into a portion caused by external physical nongravitational forces and into a temperature component. Due to the atmospheric drag, the observed accelerometer signal is strongest by an order of magnitude in the along-track direction. As the science objectives focus on the atmospheric density and winds, first efforts supported by ESA to process Swarm accelerometer data for their scientific exploitation were directed towards the along-track component of Swarm C (Siemes et al., 2016).

Space accelerometers of similar design flew aboard recent gravity field missions CHAMP, GRACE and GOCE (for more information and references, see e.g. Bezděk et al., 2014). From these missions, the character of Swarm accelerometer data is closest to that of GRACE (all three accelerometer components observed, similar altitude and signal magnitude); because of this, we use the GRACE accelerometer data sometimes as a reference. Accelerometer data from CHAMP and GRACE were also a subject of many calibration studies (e.g. Bezděk, 2010; Gruber et al., 2005; Klinger and Mayer-Gürr, 2016; van den IJssel and Visser, 2007; Kim and Tapley, 2015; Weigelt and Sneeuw, 2005).

A specific feature in the calibration of the Swarm accelerometer data is a typically quite important contribution of the onboard temperature variation. To this purpose, we have developed a so-called *linear temperature correction*, which was demonstrated to be capable of correcting the accelerometer data for temperature dependence in the process of validation against the modelled nongravitational forces (Bezděk et al., 2017). In the current paper, it is our goal to show that this approach provides good results in the GPS-based calibration as well, fully independent of nongravitational models. Our calibrated accelerometer curves will be compared to those released by ESA, where the temperature correction algorithm is different (Siemes et al., 2016).

First, the calibration method will be described and illustrated on simulated data (Section 2). Then we will apply the method to real data of Swarm A and Swarm C, comparing the results also with GRACE (Section 3). Finally, Section 4 provides long-term statistical results for the application of the presented calibration method to the last ESA release of the calibrated Swarm C accelerometer data covering the period from July 2014 to April 2016.

1.1. Acceleration approach

A straightforward method to derive parameters of a particular force from the observed motion of a test body via Newton's second law has been used in physics probably since the very Newton's times. More recently, the use of higher flying satellites that observe a lower flying satellite in order to improve the high-frequency part of the gravity field was discussed by Rummel (1975, 1979) or Douglas et al. (1980). Within the global gravity field modelling, this observational model is called *high-low satellite-to-satellite tracking*; using the GPS positioning of a lower-flying satellite, first substantially improved global Earth gravity field models were obtained starting with CHAMP (e.g. Reigber et al., 2003). Since then, a number of global gravity field models derived from GPS positions of gravity missions CHAMP, GRACE, GOCE and now also Swarm, have been published (Bezděk et al., 2014; Weigelt et al., 2013; Zehentner and Mayer-Gürr, 2014; Weigelt et al., 2009; Jäggi et al., 2015; Visser et al., 2014; Badura et al., 2006; Bucha et al., 2015). Within this context, the term *acceleration approach* is used for methods that formulate and solve the observation equations directly in the acceleration domain.

In our implementation of the acceleration approach, we have been using two decorrelation transformations, whose application is necessary in order to obtain estimated parameters accompanied with a corresponding uncertainty statement. We applied our methodology to the calibration of GRACE accelerometer data (Bezděk, 2010); later we modified it for estimating the gravity field coefficients (Bezděk et al., 2014).

For processing the satellite orbital data we used our own orbital propagator NUMINTSAT (Bezděk et al., 2009); the computation of the physically modelled nongravitational accelerations is described in Bezděk et al. (2017, sect.

1.1). The GPS-based accelerations were computed from the IfG kinematic orbits (Zehentner and Mayer-Gürr, 2016, 2014). As the uncalibrated Swarm C along-track accelerometer data, we used the ESA step-corrected data being a part of the ACCxCAL_2 product (Siemes et al., 2016).

1.2. Internal verification and external validation

In using the terms 'verification' and 'validation' we follow Murray-Smith (1995, 1998, 2015) who characterizes *internal verification* as the process of proving that a computer simulation is consistent with the underlying model, while *external validation* involves demonstrating that the mathematical model has an acceptable accuracy over the range of conditions relevant for the application. These definitions emphasize clearly that the processes that lead to internal verification should provide proof of the internal consistency and accuracy of the simulation program, whereas the assessment of external validity of the model involves questions of judgment to a greater extent (Murray-Smith, 1995).

Perhaps more practically, according to Vallado (2007), we *verify* our implementation against existing data or results (ensure it is coded properly), while we *validate* that the model accurately reflects the truth.

In this respect, our previous paper Bezděk et al. (2017) dealt with an external validation of Swarm accelerometer data by physically modelled nongravitational accelerations, while in the present paper the implemented calibration model is first verified through simulated data (Section 2.2) and then the calibration results are validated against independent data sets (Section 3 and 4).

2. Calibration method

Our calibration method is based on *Newton's second law* of motion, which we express in terms of accelerations,

$$\boldsymbol{a}^{\mathrm{GPS}} \approx \frac{d^2\boldsymbol{r}}{dt^2} = \boldsymbol{a}_{\mathrm{geop}} + \boldsymbol{a}_{\mathrm{LS}} + \boldsymbol{a}_{\mathrm{TID}} + \boldsymbol{a}_{\mathrm{ETC}} + \boldsymbol{a}_{\mathrm{NG}}. \tag{1}$$

On the right-hand side, there are the main forces acting on the satellite in a low Earth orbit (below 2000 km), namely gravitational acceleration due to the geopotential $\boldsymbol{a}_{\mathrm{geop}}$, (direct) lunisolar perturbations $\boldsymbol{a}_{\mathrm{LS}}$, acceleration due to solid Earth and ocean tides $\boldsymbol{a}_{\mathrm{TID}}$, correction $\boldsymbol{a}_{\mathrm{ETC}} = \boldsymbol{a}_{\mathrm{REL}} + \boldsymbol{a}_{\mathrm{AOD}}$ due to general relativity $\boldsymbol{a}_{\mathrm{REL}}$ and atmospheric and oceanic non-tidal effects $\boldsymbol{a}_{\mathrm{AOD}}$, nongravitational accelerations $\boldsymbol{a}_{\mathrm{NG}}$. On the left-hand side, there is the actual motion of the satellite, represented as the second derivative of the position vector $\boldsymbol{r}$ of the satellite's centre of mass. The GPS receiver of each Swarm satellite produces a time series of its positions $\boldsymbol{r}$ with a constant time step. By means of a numerical derivative of this time series, one can get a time series of GPS-based accelerations $\boldsymbol{a}^{\mathrm{GPS}}$ which approximate the real accelerations $d^2\boldsymbol{r}/dt^2$. Using $\boldsymbol{a}^{\mathrm{GPS}}$ computed at each orbital position $\boldsymbol{r}$, Eq. (1) thus allows us to estimate one or more accelerations on the right-hand side, the remaining acceleration terms are supposed to be known. (For more information on approximating $d^2\boldsymbol{r}/dt^2$ by the numerical derivative, refer to Section 2.1 and 2.2 in Bezděk et al., 2014.)

If one assumes that all the acceleration terms of gravitational origin $\boldsymbol{a}_{\mathrm{GRAV}}$ are known (or precisely modelled), then for the centre of mass, it is possible to obtain a *GPS-based nongravitational acceleration*

$$\boldsymbol{a}_{\mathrm{NG}}^{\mathrm{GPS}} = \boldsymbol{a}^{\mathrm{GPS}} - (\boldsymbol{a}_{\mathrm{geop}} + \boldsymbol{a}_{\mathrm{LS}} + \boldsymbol{a}_{\mathrm{TID}} + \boldsymbol{a}_{\mathrm{ETC}}) \equiv \boldsymbol{a}^{\mathrm{GPS}} - \boldsymbol{a}_{\mathrm{GRAV}}. \tag{2}$$

The time series of these accelerations exhibits solely the action of nongravitational forces, which should be measured by an accelerometer. The location of the accelerometers relative to the centre of mass of the Swarm spacecraft is within a few millimetres in the cross-track and radial directions, and within 1–2 cm in the along-track direction (Ch. Siemes, priv. comm.). It can be shown that the inertial forces induced by these offsets are negligible compared to the along-track nongravitational signal (2) treated in this paper.

2.1. Calibration equation

At each point of the satellite orbit we define a *calibration equation*

$$a_{\mathrm{NG}}^{\mathrm{GPS}} = B + S \cdot a_{\mathrm{ACC}}^{\mathrm{UNCAL}} + Q \cdot T(t+F) + G \cdot (t - t_0) + \epsilon, \tag{3}$$

where B is the bias, S scale factor, $a_{\mathrm{ACC}}^{\mathrm{UNCAL}}$ uncalibrated accelerometer data in a given component. The linear temperature correction is represented by the temperature factor Q which multiplies the temperature signal $T(t+F)$ with a time shift F. Finally, there is a trend term $G \cdot (t - t_0)$ with time t reckoned from an arbitrary origin t_0 and the statistical noise ϵ. In Eq. (3), we use the nongravitational accelerations (2) derived from GPS positions as the calibration standard, we use the projection $a_{\mathrm{NG}}^{\mathrm{GPS}}$ of this vector in the direction of the accelerometer data component being calibrated (e.g. along-track). We look for the calibration parameters B, S, Q, G by solving the linear system (3); we do so by the linear least-squares method taking into account the correlated errors in GPS positions (Bezděk, 2010, sec. 4). The calibrated accelerometer curve is then obtained as the fitted function, namely

$$a_{\mathrm{ACC}}^{\mathrm{CAL}} = \hat{B} + \hat{S} \cdot a_{\mathrm{ACC}}^{\mathrm{UNCAL}} + \hat{Q} \cdot T(t+F) + \hat{G} \cdot (t - t_0), \tag{4}$$

where the estimated values of the linear calibration parameters are marked with a hat (cf. Bezděk, 2010, App. A). (We note that in practice, the term ϵ contains all sources of measurements noise and calibration model errors in Eq. 3.)

2.2. Verification of the calibration method by simulated data

Fig. 1 shows an example of calibrating simulated accelerometer data. We computed the precise satellite positions over a segment of five satellite revolutions, to these positions we added the noise comparable in its statistical properties to the real case (for technical details, refer to Section 2.2.1). In Fig. 1a, each point represents a GPS-based nongravitational acceleration $a_{\mathrm{NG}}^{\mathrm{GPS}}$ in the along-track component. As already discussed by Bezděk (2010), a few centimetres correlated noise in GPS positions produces a rather huge noise in accelerations, at the 10^{-5} m·s^{-2} level. In the present case, the modelled nongravitational accelerations are lower by two orders of magnitude. Fig. 1b is a zoom on the y-axis of the same data, now the acceleration curves become visible. The simulated satellite motion took into account the modelled nongravitational accelerations $a_{\mathrm{NG}}^{\mathrm{MOD}}$, which play the role of the 'true' nongravitational signal (red dashed). The uncalibrated accelerometer readouts $a_{\mathrm{NG}}^{\mathrm{UNCAL}}$ (cyan) were simulated to represent the perturbations present in the real calibration Eq. (3). Namely, to a shifted and scaled copy of the true signal $a_{\mathrm{w/t\,T}}^{\mathrm{UNCAL}}$ (magenta) caused by a nonzero bias and a scale factor, we added a sinusoidal temperature variation T (green). We are looking for the calibration parameters defined in Eq. (3) that would reshape the 'measured' uncalibrated curve $a_{\mathrm{NG}}^{\mathrm{UNCAL}}$ (cyan) into the calibrated curve $a_{\mathrm{NG}}^{\mathrm{CAL}}$ (blue), which should be close to the original signal $a_{\mathrm{NG}}^{\mathrm{MOD}}$ (red dashed). As mentioned in Section 1.1, double decorrelation of the linear system (3) is necessary for a correct estimate of the uncertainty band (light blue). The sought original curve $a_{\mathrm{NG}}^{\mathrm{MOD}}$ (red) is indeed located inside the uncertainty band (light blue), which is defined at each point as a confidence interval with a coverage factor 3 ('three-sigma rule', a confidence level of 99.7%, used throughout this paper).

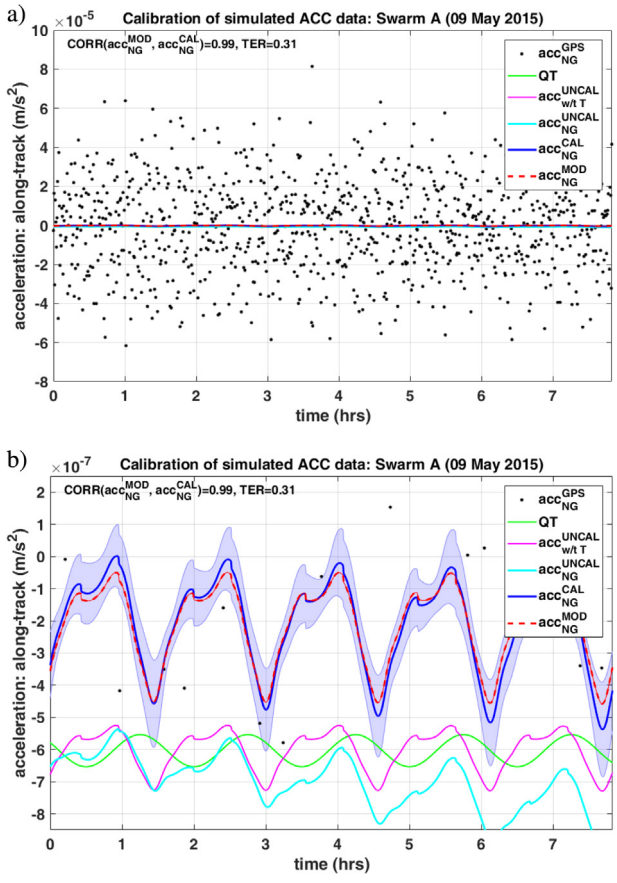

Fig. 1. Calibration of simulated accelerometer data. Each point represents GPS-based nongravitational acceleration $a_{\mathrm{NG}}^{\mathrm{GPS}}$. Simulated data cover five revolutions of Swarm A on 9 May 2015. The function CORR provides the correlation coefficient between its two arguments. The abbreviation TER stands for temperature-energy ratio, which will be discussed in Section 3. Refer to the text for further details.

2.2.1. Technical details of the simulation

In Fig. 1, we computed the precise satellite positions over an orbit segment of five revolutions with a time step of 30 s, starting from the real Swarm A orbital elements (in May 2015 the mean altitude of Swarm A was about 450 km). The only simulated acceleration of gravitational origin was a 5 × 5 gravity field, but this is not much important, as $\boldsymbol{a}_{\mathrm{GRAV}}$ is subtracted, cf. Eq. (2). As for the noise, following our previous analyses (Bezděk et al., 2014, sect. 2.4) we modelled the noise in the GPS positions as correlated, namely as a first-order autoregressive process with an autocorrelation of 0.99. The 'true' nongravitational signal (red dashed) was modelled as a sum of atmospheric drag and direct solar radiation pressure. The uncalibrated accelerometer readouts (cyan) were obtained via a priori calibration parameters: $\mathrm{F} = -1.75$ h, $\mathrm{S} = 2$, $\mathrm{B} = 1.2 \times 10^{-6}$ m·s^{-2}, $\mathrm{G} = 5 \times 10^{-8}$, $\mathrm{Q} = -1 \times 10^{-7}$ m·s^{-2}/°C. As already mentioned in the Introduction, our calibration method is described in the two previous publications Bezděk (2010) and Bezděk et al. (2014).

3. Calibration of Swarm accelerometer data including temperature correction

As mentioned in Section 1, for the Swarm satellites the physical nongravitational signal is strongest in the along-track direction, where the atmospheric drag is dominant. Although the Swarm accelerometers measure in all three axes of the satellite reference frame, in this paper we will calibrate and discuss only the along-track component. (We note that the calibration of other accelerometer components can be done in the same way.)

Fig. 2 shows the calibration of the Swarm C accelerometer data. By means of the fitted calibration parameters, the uncalibrated accelerometer curve $a_{\mathrm{ACC}}^{\mathrm{UNCAL}}$ (cyan) was shifted, scaled and reshaped into the calibrated accelerometer curve $a_{\mathrm{ACC}}^{\mathrm{CAL}}$ (blue). The uncertainty band (light transparent blue) along the calibrated curve indicates where the true accelerometer value should be located at a high level of confidence; this uncertainty estimate is based solely

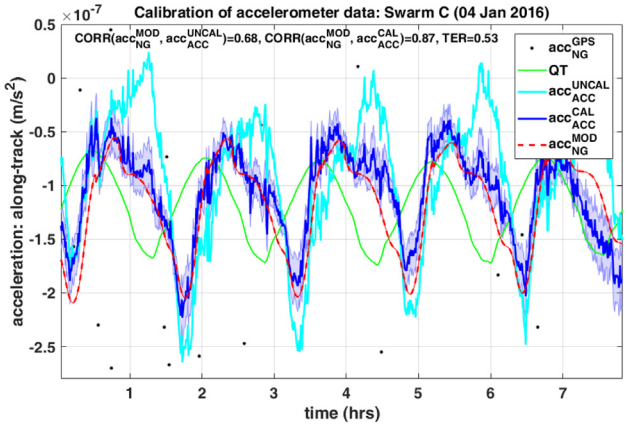

Fig. 2. Calibration of real accelerometer data of Swarm C (4 Jan 2016; along-track component).

on the noise in GPS positions. (For this reason, our uncertainty estimate may provide only a lower bound for the total uncertainty.)

The calibrated accelerometer curve $a_{\mathrm{ACC}}^{\mathrm{CAL}}$ (blue) and the modelled physical nongravitational accelerations $a_{\mathrm{NG}}^{\mathrm{MOD}}$ (red) were computed in a completely independent way. Therefore, the modelled nongravitational accelerations (red) may be used as an external validation tool. After subtracting the parasitical signal due to the onboard temperature variations (green) from the uncalibrated accelerometer signal (cyan), the correspondence between the calibrated accelerometer curve (blue) and the modelled nongravitational accelerations (red) visibly improved. This visual impression can be quantified, the coefficient of correlation 0.68 before the calibration increased to 0.87 after the calibration. This improved correlation was brought about by the positive effect of the linear temperature correction. If the calibrated data and the modelled nongravitational accelerations agree at a satisfactory level, the importance of including the temperature correction could be quantified by the temperature-energy ratio (Bezděk et al., 2017). Temperature-energy ratio is defined as the quotient of the energy in the fitted temperature curve divided by the energy in the modelled nongravitational accelerations. For the data in Fig. 2, the temperature-energy ratio is 0.53, which means that the energy in the temperature correction curve $\hat{Q}\cdot T$ (green) represents 53% of the energy in the modelled nongravitational accelerations (red). In this case, the linear temperature correction can hardly be neglected (as in Figs. 3c and 4 below).

3.1. Accelerometer data of GRACE and Swarm A/C

In May 2015, the orbital planes of the lower satellite pair Swarm A/C and that of GRACE A/B were approximately aligned. However, there was a half revolution difference between the two pairs, and also the altitude of Swarm A/C at 460 km was higher compared to that one of GRACE A/B at 400 km. Fig. 3a shows the calibrated

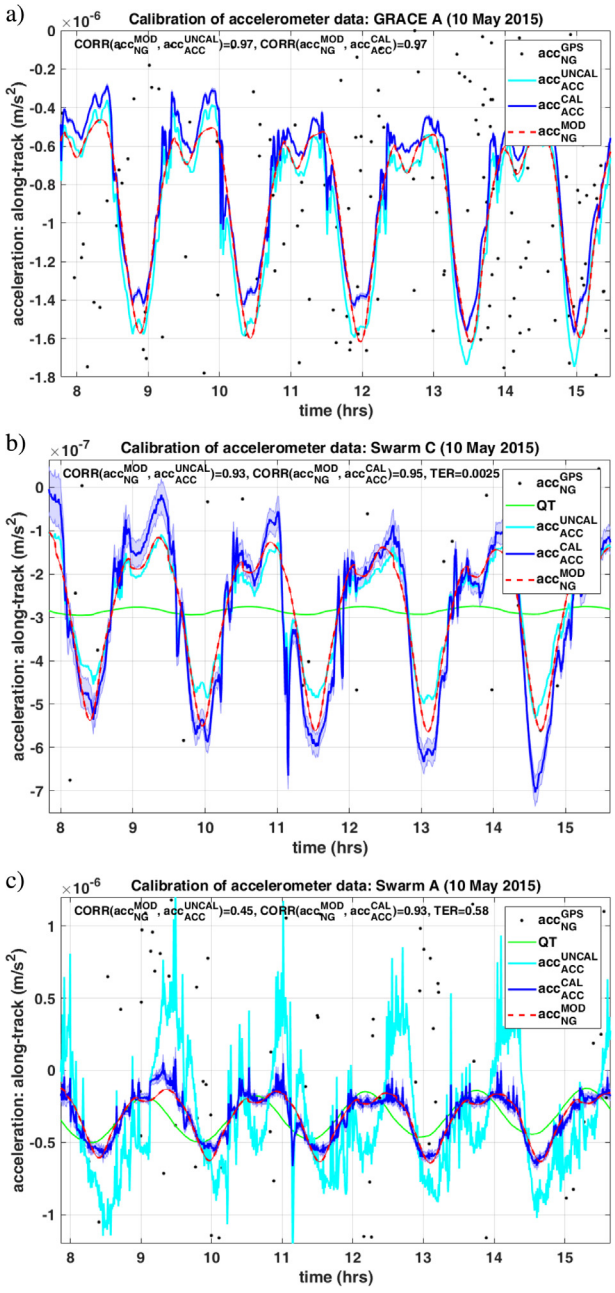

Fig. 3. Calibration of real accelerometer data: (a) GRACE A, (b) Swarm C, (c) Swarm A (10 May 2015; along-track component).

accelerometer curve for GRACE A. Here, the calibration method is the same, only no temperature correction has been applied; the correlation between both uncalibrated and calibrated accelerometer data with modelled nongravitational accelerations has the same high value of 0.97. The curve of the calibrated accelerometer data of Swarm C in Fig. 3b is also well correlated with modelled nongravitational accelerations, its coefficient of correlation being 0.95. For Swarm C, the temperature-energy ratio is close to zero, thus in the calibration virtually no temperature correction was used. In contrast, the temperature-energy ratio of 0.58 for Swarm A means that for the accelerometer

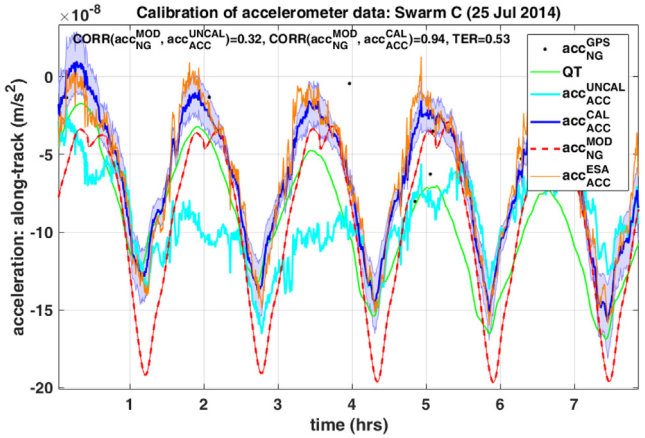

Fig. 4. The linear temperature correction and the ESA temperature correction for the Swarm C accelerometer data (25 July 2014).

data in Fig. 3c, including the temperature correction was significant. This is confirmed by the substantial increase in the correlation between the modelled accelerations and the uncalibrated accelerometer data of 0.45–0.93 after the calibration.

The three panels of Fig. 3 show a very similar character of the accelerometer signals sensed by GRACE A and Swarm A/C. Although GRACE A flew at a somewhat lower altitude compared to Swarm A/C, all three calibrated waveforms clearly share common features; namely an increased drag at perigee and noticeable spikes at the terminator crossings. Here, the modelled nongravitational accelerations (i) are computed independently from all calibrated data; (ii) provide a much smoother a priori version of the real nongravitational signal; (iii) serve as an intermediary between the three calibrated accelerometer curves. Thus, the agreement of the modelled nongravitational signal with the calibrated accelerometer signal of each Swarm A and Swarm C separately implies the agreement of the calibrated signals of Swarm A and Swarm C themselves.

4. Comparison of the linear temperature correction with that released by ESA

Similar to previous figures, Fig. 4 shows the calibrated along-track accelerometer data of Swarm C. Here the inclusion of the linear temperature corrective term substantially improved the correlation of the accelerometer data with models (red[1]), from 0.32 for uncalibrated accelerometer data (cyan) to 0.94 for calibrated accelerometer data (blue). To the figure we added the graph of the accelerometer data a^{ESA}_{ACC} released by ESA (orange), where a different temperature correction was used (Siemes et al., 2016). As already mentioned, our goal is to calibrate the accelerometer data including the uncertainty estimate of each accelerometer measurement. In fact, the statement where we expect the true acceleration value to be located is at best conveyed by the corresponding confidence interval; the true value should be *anywhere* within the confidence interval at a given confidence level (99.7% in our case). And in this respect, it is very good to see that the ESA-calibrated accelerometer curve (orange) mostly falls within the uncertainty band (light blue), or that it is at least close to it. In this example, the validation by independent physically modelled nongravitational accelerations is positive; the correlation coefficients are high, 0.94 between the ESA-calibrated data and physical models, and 0.98 between the linear-temperature-corrected curve and the ESA-calibrated curve. As it is obvious visually, including the temperature corrective term in the calibration is indeed important, for the data in Fig. 4 the temperature-energy ratio is 0.53.

In Figs. 2–4 we showed the calibration results for step-corrected Swarm C along-track accelerometer data by picking three different dates over the years 2014–2016. These figures are typical for periods, when the presented linear temperature correction worked satisfactorily, which happened for the majority of the available Swarm C data (more details in the next section). Thus for example also the ESA-released accelerometer data produced graphs very close to those of our calibrated data displayed in Figs. 2 and 3b. As for the length of the calibration segment, similar results were obtained for segments covering 2–6 revolutions, and this is positive, the calibration results should not depend too much on the segment length. On the other hand, the contribution of temperature to the calibrated curve may change quite a lot, it was 53 % in Fig. 2 vs. 0.25% in Fig. 3b. And this varying contribution is also rather typical (Fig. 5 in the next section provides more details).

4.1. Validation of ESA accelerometer data covering two years

Recently, ESA released a new data set of Swarm accelerometer observations, which are determined through a combination of the nongravitational acceleration derived from the GPS receiver and the calibrated accelerometer data (Siemes et al., 2016). The new data set covers the period from 19 July 2014 to 27 April 2016 and provides scientific users with the along-track component of the Swarm C accelerometer data (ACCxCAL_2, baseline 02; http://earth.esa.int/swarm/).

We validated this data set over individual 5-revolution segments. We say that two signals have similar waveforms at an acceptable level, when their respective coefficient of correlation is greater than a limiting value of 0.85 (Bezděk et al., 2017, sect. 3.3). In particular, the physically modelled accelerations serve here as an independent validation tool (shown in red in the previous figures). For the signals shown in Fig. 4, the uncalibrated accelerometer signal (cyan) is not validated by modelled accelerations

[1] For interpretation of color in 'Figs. 1–5', the reader is referred to the web version of this article.

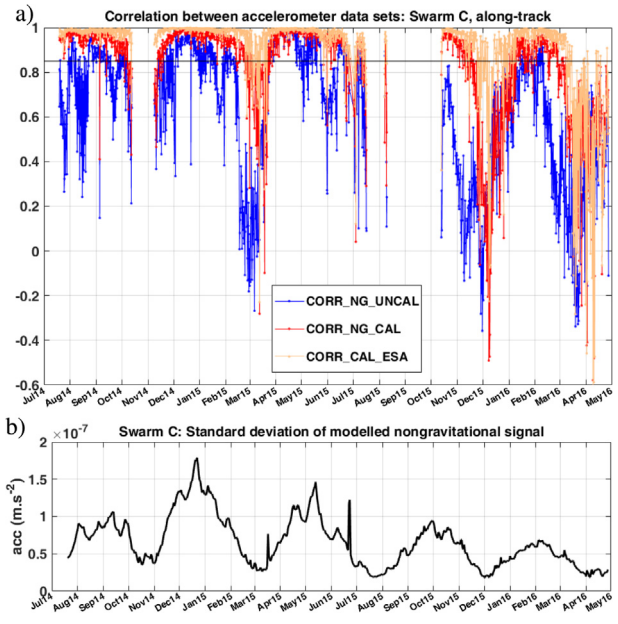

Fig. 5. Comparison of the linear temperature correction with the ESA-devised temperature correction. (a) Cross-validation of both the temperature corrections over almost two years of Swarm C data (Jul 2014–Apr 2016). (b) Variability of the accelerometer signal estimated by the standard deviation of the modelled nongravitational accelerations.

(correlation $0.32 < 0.85$), while both our calibrated (blue) and ESA-calibrated accelerations are validated (correlation $\geqslant 0.85$). We note that there is no problem if the physically modelled accelerations are shifted vertically a bit with respect to the calibrated accelerations (as in Fig. 4); the presence of slowly changing bias in modelled nongravitational accelerations has been also identified in the GRACE A accelerometer data (Bezděk, 2010, sect. 5.2). We guess that this bias may be attributed to a systematic component of the uncertainty in the atmospheric density models.

In Fig. 5a, each point represents the coefficient of correlation between the respective signals over one segment. There are several longer time intervals, when the uncalibrated accelerations do not correspond well in their waveforms to modelled accelerations (blue curve). On including the linear temperature correction (described in Section 2), the percentage of validated accelerometer data clearly increased (red curve). We tested also the correspondence of the waveforms between the ESA-calibrated accelerations and models, but the most interesting is the correlation between the waveforms of our temperature-corrected accelerations and those released by ESA (light orange curve). A decrease in the correlation points towards the end of the shown time period (March and April 2016, and to a lesser extent in March and December 2015), can be explained by a declining variability of the external nongravitational signal due to a gradual approach of the 11-year solar activity cycle to its minimum (to be reached around 2019). The accelerometer signal variability is represented in Fig. 5b as the standard deviation of the modelled nongravitational accelerations over one satellite revolution.

We note also that there are periods when the nongravitational signal variability is low; for these periods the coefficient of correlation is obviously not a good measure of correspondence between different nongravitational signals, the fluctuating part of the signal quantified by the standard deviation is reduced (cf. Bezděk et al., 2017). As Fig. 5b indicates, this happens when the solar cycle approaches the minimum of its 11-year cycle (around 2019).

From the perspective of validating the ESA temperature-corrected Swarm C accelerometer data, we may say that in total 87% of the data segments are validated by our calibrated accelerations and/or by physical models. This is comparable to 85% of the GRACE A accelerometer data validated by physical models (over a reference period in 2002–2003 with a similar accelerometer signal variability). The rest of the ESA accelerometer data cannot be evaluated by our method. We note that the relatively high percentage of the validated ESA accelerometer data is related to the fact that the periods with problematic accelerometer data were not released (data gaps in Fig. 5a). It is also interesting to remark that the linear temperature correction was necessary in about 50% of the validated cases, and in these cases the mean temperature-energy ratio was 0.8 (i.e. the fitted temperature correction contains on average 80% of the energy in the modelled accelerations).

To characterize the uncertainty of the obtained calibrated accelerations, in each segment covering five orbital revolutions, we calculated the median of its uncertainty band. For both studied 2-year long stretches of the tested accelerometer data of Swarm C and GRACE A, the histograms of these medians take approximately Gaussian form, when they are expressed as logarithms (Bezděk, 2007, 2010). This way, we can characterize the mean standard error (one sigma) of the calibrated accelerometer data of GRACE A to be 3.7 $\mathrm{nm{\cdot}s^{-2}}$, and that of Swarm C to be 5.4 $\mathrm{nm{\cdot}s^{-2}}$ (this is a preliminary averaged value). Due to a greater GPS noise, the mean uncertainty of the calibrated Swarm C accelerometer data is worse by a factor of 1.5 compared to a reference GRACE A accelerometer data set.

5. Conclusions and outlook

In this paper, we presented the first results on the application of our GPS-based calibration procedure to the Swarm accelerometer data, which have a special feature by being considerably disturbed by the onboard temperature variation. Over several example segments, each covering five satellite revolutions, we obtained meaningful calibrated measurements for the along-track component of the accelerometer data of Swarm A, Swarm C and GRACE A. Using the physically modelled nongravitational accelerations as an independent external validation tool, we demonstrated that the calibration procedure is capable of producing consistent accelerometer measurements for all three studied satellites, each calibrated value

being accompanied by a corresponding uncertainty estimate. Finally, we pointed out a good agreement between the calibrated accelerometer measurements by our approach and those processed by ESA where the use was made of a different temperature corrective algorithm. We showed that nearly 90% of the ESA calibrated accelerometer data covering almost 2 years are validated by our calibrated accelerometer data or modelled nongravitational accelerations. The mean uncertainty of our calibrated along-track accelerometer data of Swarm C over this period was found to be around 5.4 $\mathrm{nm \cdot s^{-2}}$.

The presented results are useful for further work with the Swarm accelerometer data. It is encouraging that for the majority of the data segments the two analysed independent temperature correction methods produced very similar calibrated data. Unfortunately, besides the parasitic temperature influence, the Swarm accelerometer data contain a lot of hardware related anomalies and steps; hence, the number of the correctly calibrated data depends among other things on the application of the step-corrective algorithm developed by ESA, which so far has been applied to the released along-track accelerometer component of Swarm C. In any case, this paper supports the idea that at least for some selected longer time periods the Swarm accelerometer data can be calibrated and made thus available for further scientific use.

Acknowledgements

This work was supported by projects LG15003 and RVO: 67985815. The authors acknowledge ESA for all Swarm related data and NASA JPL and ESA for all GRACE data. The authors thank C. Siemes and other three anonymous reviewers for their careful reading and helpful suggestions.

References

Badura, T., Sakulin, C., Gruber, C., Klostius, R., 2006. Derivation of the CHAMP-only global gravity field model TUG-CHAMP04 applying the energy integral approach. Stud. Geophys. Geod. 50, 59–74. https://doi.org/10.1007/s11200-006-0002-3.

Bezděk, A., 2007. Lognormal distribution of the observed and modelled neutral thermospheric densities. Stud. Geophys. Geod. 51, 461–468. https://doi.org/10.1007/s11200-007-0027-2.

Bezděk, A., 2010. Calibration of accelerometers aboard GRACE satellites by comparison with POD-based nongravitational accelerations. J. Geodyn. 50, 410–423. https://doi.org/10.1016/j.jog.2010.05.001.

Bezděk, A., Klokočník, J., Kostelecký, J., Floberghagen, R., Gruber, C., 2009. Simulation of free fall and resonances in the GOCE mission. J. Geodyn. 48, 47–53. https://doi.org/10.1016/j.jog.2009.01.007.

Bezděk, A., Sebera, J., Encarnação, J., Klokočník, J., 2016. Time-variable gravity fields derived from GPS tracking of Swarm. Geophys. J. Int. 205, 1665–1669. https://doi.org/10.1093/gji/ggw094.

Bezděk, A., Sebera, J., Klokočník, J., 2017. Validation of Swarm accelerometer data by modelled nongravitational forces. Adv. Space Res. 59, 2512–2521. https://doi.org/10.1016/j.asr.2017.02.037.

Bezděk, A., Sebera, J., Klokočník, J., Kostelecký, J., 2014. Gravity field models from kinematic orbits of CHAMP, GRACE and GOCE satellites. Adv. Space Res. 53, 412–429. https://doi.org/10.1016/j.asr.2013.11.031.

Bruinsma, S.L., Doornbos, E., Bowman, B.R., 2014. Validation of GOCE densities and evaluation of thermosphere models. Adv. Space Res. 54, 576–585. https://doi.org/10.1016/j.asr.2014.04.008.

Bucha, B., Bezděk, A., Sebera, J., Janák, J., 2015. Global and regional gravity field determination from GOCE kinematic orbit by means of spherical radial basis functions. Surv. Geophys. 36, 773–801. https://doi.org/10.1007/s10712-015-9344-0.

Dahle, C., Arnold, D., Jäggi, A., 2017. Impact of tracking loop settings of the Swarm GPS receiver on gravity field recovery. Adv. Space Res. 59, 2843–2854. https://doi.org/10.1016/j.asr.2017.03.003.

Douglas, B.C., Goad, C.C., Morrison, F.F., 1980. Determination of the geopotential from satellite-to-satellite tracking data. J. Geophys. Res. 85, 5471–5480. https://doi.org/10.1029/JB085iB10p05471.

Encarnação, J., Arnold, D., Bezděk, A., Dahle, C., Doornbos, E., van den IJssel, J., Jäggi, A., Mayer-Gürr, T., Sebera, J., Visser, P., Zehentner, N., 2016. Gravity field models derived from Swarm GPS data. Earth Planets Space 68, 127. https://doi.org/10.1186/s40623-016-0499-9.

Friis-Christensen, E., Lühr, H., Knudsen, D., Haagmans, R., 2008. Swarm – an Earth observation mission investigating geospace. Adv. Space Res. 41, 210–216. https://doi.org/10.1016/j.asr.2006.10.008.

Gruber, C., Tsoulis, D., Sneeuw, N., 2005. CHAMP accelerometer calibration by means of the equation of motion and an a-priori gravity model. Z. Geod. Geoinform. Landmanage. 130, 92–98 <http://geo-daesie.info/zfv/heftbeitrag/1271>.

van den IJssel, J., Visser, P., 2007. Performance of GPS-based accelerometry: CHAMP and GRACE. Adv. Space Res. 39, 1597–1603. https://doi.org/10.1016/j.asr.2006.12.027.

Jäggi, A., Bock, H., Meyer, U., Beutler, G., van den IJssel, J., 2015. GOCE: assessment of GPS-only gravity field determination. J. Geod. 89, 33–48. https://doi.org/10.1007/s00190-014-0759-z.

Kim, J., Tapley, B.D., 2015. Estimation of non-gravitational acceleration difference between two co-orbiting satellites using single accelerometer data. J. Geod. 89, 537–550. https://doi.org/10.1007/s00190-015-0796-2.

Klinger, B., Mayer-Gürr, T., 2016. The role of accelerometer data calibration within GRACE gravity field recovery: results from ITSG-Grace2016. Adv. Space Res. 58, 1597–1609. https://doi.org/10.1016/j.asr.2016.08.007.

Murray-Smith, D., 1995. Continuous System Simulation. Springer-Science+Business Media. https://doi.org/10.1007/978-1-4615-2504-2.

Murray-Smith, D.J., 1998. Methods for the external validation of continuous system simulation models: a review. Math. Comput. Modell. Dyn. Syst. 4, 5–31. https://doi.org/10.1080/13873959808837066.

Murray-Smith, D.J., 2015. Testing and Validation of Computer Simulation Models: Principles, Methods and Applications, first ed. Springer Publishing Company, Inc.

Olsen, N., Stolle, C., Floberghagen, R., Hulot, G., Kuvshinov, A., 2016. Special issue "Swarm science results after 2 years in space". Earth Planets Space 68, 172. https://doi.org/10.1186/s40623-016-0546-6.

Reigber, C., Schwintzer, P., Neumayer, K.H., Barthelmes, F., König, R., Förste, C., Balmino, G., Biancale, R., Lemoine, J.M., Loyer, S., Bruinsma, S., Perosanz, F., Fayard, T., 2003. The CHAMP-only earth gravity field model EIGEN-2. Adv. Space Res. 31, 1883–1888. https://doi.org/10.1016/S0273-1177(03)00162-5.

Rummel, R., 1975. Downward Continuation of Gravity Information from Satellite to Satellite Tracking or Satellite Gradiometry in Local Areas. Technical Report. Ohio State University, Reports of the Department of Geodetic Science, No. 221.

Rummel, R., 1979. Determination of short-wavelength components of the gravity field from satellite-to-satellite tracking or satellite gradiometry. Manuscripta Geod. 4, 107–148.

Siemes, C., de Teixeira da Encarnação, J., Doornbos, E., van den IJssel, J., Kraus, J., Pešty, R., Grunwaldt, L., Apelbaum, G., Flury, J., Holmdahl Olsen, P.E., 2016. Swarm accelerometer data processing

from raw accelerations to thermospheric neutral densities. Earth Planets Space 68, 92. https://doi.org/10.1186/s40623-016-0474-5.

Vallado, D.A., 2007. Fundamentals of Astrodynamics and Applications. Microcosm Press and Springer.

Visser, P., Doornbos, E., van den IJssel, J., Teixeira da Encarnação, J., 2013. Thermospheric density and wind retrieval from Swarm observations. Earth Planets Space 65, 1319–1331. https://doi.org/10.5047/eps.2013.08.003.

Visser, P., van der Wal, W., Schrama, E., van den IJssel, J., Bouman, J., 2014. Assessment of observing time-variable gravity from GOCE GPS and accelerometer observations. J. Geod. 88, 1029–1046. https://doi.org/10.1007/s00190-014-0741-9.

Weigelt, M., Dam, T., Jäggi, A., Prange, L., Tourian, M.J., Keller, W., Sneeuw, N., 2013. Time-variable gravity signal in Greenland revealed by high-low satellite-to-satellite tracking. J. Geophys. Res. (Solid Earth) 118, 3848–3859. https://doi.org/10.1002/jgrb.50283.

Weigelt, M., Sideris, M.G., Sneeuw, N., 2009. On the influence of the ground track on the gravity field recovery from high-low satellite-to-satellite tracking missions: CHAMP monthly gravity field recovery using the energy balance approach revisited. J. Geod. 83, 1131–1143. https://doi.org/10.1007/s00190-009-0330-5.

Weigelt, M., Sneeuw, N., 2005. Numerical velocity determination and calibration methods for CHAMP using the energy balance approach. In: Jekeli, C., Bastos, L., Fernandes, J. (Eds.), Gravity, Geoid and Space Missions. International Association of Geodesy Symposia, vol. 129. Springer, Berlin, Heidelberg, pp. 54–59. https://doi.org/10.1007/3-540-26932-0_10.

Xiong, C., Stolle, C., Lühr, H., 2016. The Swarm satellite loss of GPS signal and its relation to ionospheric plasma irregularities. Space Weather 14, 563–577. https://doi.org/10.1002/2016SW001439.

Zehentner, N., Mayer-Gürr, T., 2014. New approach to estimate time variable gravity fields from high-low satellite tracking data. In: Marti, U. (Ed.), Gravity, Geoid and Height Systems. Springer International Publishing, pp. 111–116. https://doi.org/10.1007/978-3-319-10837-7_14.

Zehentner, N., Mayer-Gürr, T., 2016. Precise orbit determination based on raw GPS measurements. J. Geod. 90, 275–286. https://doi.org/10.1007/s00190-015-0872-7.